Effects of the rare-earth ions on some properties of a nickel-zinc ferrite

1994 J. Phys.: Condens. Matter 6 5707

(http://iopscience.iop.org/0953-8984/6/29/013)

J. Phys.: Condens. Matter 6 (1994) 5707–5716. Printed in the UK

Effects of the rare-earth ions on some properties of a nickel–zinc ferrite

N Rezlescu, E Rezlescu, C Pasnicu and M L Craus
Institute of Technical Physics, Splai Bahlui 47, 6600 Jassy, Romania

Received 30 November 1993, in final form 1 February 1994

Abstract. The effect of Fe substitutions by rare-earth ions on magnetic and electrical properties of a Ni–Zn ferrite prepared by the classical method is investigated. A set of seven compounds with formula $Ni_{0.7}Zn_{0.3}Fe_{1.98}R_{0.02}O_4$, where R ≡ Yb, Er, Dy, Tb, Gd, Sm or Ce, was prepared. Emphasis is placed on current experimental results of bulk magnetic measurements and transport phenomena. The results obtained reveal that, by introducing a relatively small amount of R_2O_3 instead of Fe_2O_3, an important modification of both the structure and the magnetic and electrical properties can be obtained. We explain the influence of the rare-earth ions as an effect of the ionic radius. This assumption is supported by the lattice constant measurements. The best results from the viewpoint of magnetic and electrical characteristic acceptable for high frequencies were obtained for R ions with a large radius and with a stable valence of 3+ such as Gd in our work.

1. Introduction

Ni–Zn polycrystalline ferrites are low-cost materials that are attractive for microwave device applications owing to their high resistivity, mechanical hardness, high Curie temperature and chemical stability. Indeed, they can be prepared easily by ceramic standard technology. In this case, the technological problem consists, mainly, in the practical possibility of avoiding discontinuous growth of the grains, assuring at the same time a high density in the final material.

In this connection, in earlier papers [1, 2], we investigated the effect of some additives and substitutions on the properties of Ni–Zn ferrites required for the high-frequency technique. In particular, we investigated the effect on the porosity. We found that, by introducing properly chosen additives or substitutes, one can realize a compromise between the properties, making it therefore possible to obtain, by the classical method, Ni–Zn ferrites, with properties beneficial for a high operating frequency.

Continuing these studies in the present paper, we have investigated the effect of rare-earth ions substituted for the iron ion in a Ni–Zn ferrite on the magnetic and electrical properties, because it is known that the rare-earth atoms R play an important role in determining the magnetocrystalline anisotropy in the 4f–3d intermetallic compounds [3–5]. No information exists in the literature about the rare-earth oxide's influence on the parameters of the ferrimagnetic oxide compounds.

It is known that the magnetic behaviour of the ferrimagnetic oxides is largely governed by the Fe–Fe interaction (the spin coupling of the 3d electrons). By introducing R ions into the spinel lattice, the R–Fe interactions also appear (3d–4f coupling), which can lead to small changes in the magnetization and Curie temperature. The R–R interactions are very weak since they result from the indirect 4f–5d–5d–4f mechanism.

Some preliminary experimental results were published in [6].

0953-8984/94/295707+10$19.50

2. Experimental details

The nominal chemical formula of the samples investigated is $Ni_{0.7}Zn_{0.3}Fe_{1.98}R_{0.02}O_4$, where R ≡ Yb, Er, Tb, Gd, Dy, Sm or Ce.

The samples were obtained by the usual ceramic technology from high-purity oxides (chemical purity greater than 99.5%). The mixing was performed in a ball mill. From this mixture at 5×10^7 N m^{-2} pressure, the toroidal forms (16 mm in outside diameter, 8 mm in inside diameter and 4 mm thick) and pellets (8 mm in diameter and 4 mm thick) were pressed. In order that all samples undergo the same heat treatment they were sintered together for the same time. The sintering was done in air in two steps: at 900 °C for 4 h and then at 1300 °C for 5 h, followed by slow cooling in air in the furnace at about 30 °C h^{-1}. Before the measurements of the magnetic and electrical properties were made, a surface layer (of about 0.3 mm thickness) of the samples, in which there might still be a zinc deficit because of volatilization during the sintering process, was removed by mechanical grinding.

The porosity of the sintered bodies was determined by measuring the Archimedes density and comparing the result with the theoretical density obtained by using precise x-ray data from polished sections.

The specific saturation magnetization σ_s was measured at liquid-nitrogen temperature (77 K) and at room temperature (293 K) with a vibrating-sample magnetometer, in a magnetic field of 8.8 kOe. A sphere of electrolytic nickel was used as standard.

The initial magnetic permeability μ_i was measured in a field of 5 mOe, at 1 kHz, by a bridge method.

The Curie points T_C were obtained from the curves of the initial permeability versus temperature.

The DC resistivity ρ at room temperature was measured with a Wheatstone bridge using silver paste contacts. From the temperature dependence of the resistivity the activation energies were determined.

Also, the Fe^{2+} ion content was established by the chemical etch method described in [7], with a precision of 0.1%.

The average grain size D_m was measured on photographs taken of lapped and etched surfaces [8], using an optical microscope Neophot Zeiss. The chemical etch was done with 70% H_3PO_4 and 30% H_2SO_4 solution, at 60–70 °C; the duration of the etch varied between 6 and 30 min.

All sintered samples were investigated by x-ray diffraction with a DRON diffractometer equipped with an iron anode.

3. Results and discussion

The experimental results concerning the x-ray analysis of the samples investigated are given in table 1.

Except for Ni–Zn ferrite without substitutions all samples contain, besides the spinel phase, a foreign phase, but in a very small amount. For some samples this was identified as the orthoferrite ($RFeO_3$). The lattice parameters were determined also; for further details on this procedure see [9].

The properties of all samples are compiled in table 2.

All results show that, by introducing a relatively small number of rare-earth ions, an important modification of both the structure and the magnetic and electrical properties can be obtained.

Table 1. Notation, chemical composition and lattice constant a for the samples studied.

Sample	Chemical composition	a (Å)	Other phases
A	$Ni_{0.7}Zn_{0.3}Fe_2O_4$	8.3687	—
Y	$Ni_{0.7}Zn_{0.3}Fe_{1.98}R_{0.02}O_4$ (R ≡ Yb)	8.3701	Foreign phase
E	$Ni_{0.7}Zn_{0.3}Fe_{1.98}R_{0.02}O_4$ (R ≡ Er)	8.3698	Orthoferrite
D	$Ni_{0.7}Zn_{0.3}Fe_{1.98}R_{0.02}O_4$ (R ≡ Dy)	8.3674	Orthoferrite
T	$Ni_{0.7}Zn_{0.3}Fe_{1.98}R_{0.02}O_4$ (R ≡ Tb)	8.3680	Orthoferrite
G	$Ni_{0.7}Zn_{0.3}Fe_{1.98}R_{0.02}O_4$ (R ≡ Gd)	8.3660	Orthoferrite
S	$Ni_{0.7}Zn_{0.3}Fe_{1.98}R_{0.02}O_4$ (R ≡ Sm)	8.3703	Foreign phase
C	$Ni_{0.7}Zn_{0.3}Fe_{1.98}R_{0.02}O_4$ (R ≡ Ce)	8.3683	Foreign phase

Table 2. Properties of the manufactured samples: rare-earth ionic radius r, specific saturation magnetization $\sigma_{77\ K}$ measured at liquid-nitrogen temperature, specific saturation magnetization $\sigma_{293\ K}$ measured at room temperature; Curie temperature T_C, initial magnetization permeability μ_i measured at room temperature, number of Fe^{2+} ions per molecule, average grain size D_m, porosity p, logarithm (electrical resistivity) $\log \rho$ and activation energy E_1.

Sample	r (Å)	$\sigma_{77\ K}$ (emu g^{-1})	$\sigma_{293\ K}$ (emu g^{-1})	T_C (°C)	μ_i	$[Fe^{2+}]$	D_m (μm)	p (%)	$\log \rho$ (Ω cm)	E_1 (eV)
A	—	97.7	67.3	415	110	0.0111	16.01	15.5	4.774	0.264
Y	0.86	93.0	65.3	410	82	0.0155	14.91	16.0	4.884	0.245
E	0.89	99.6	66.1	405	56	0.0067	14.85	13.0	4.950	0.210
D	0.92	92.1	64.8	404	78	0.0420	12.30	14.4	5.077	0.250
T	0.93	93.7	64.6	410	85	0.0677	11.70	14.2	4.960	0.221
G	0.97	103.0	65.9	410	105	0.0256	10.20	15.7	5.330	0.252
S	1.00	97.1	65.6	410	100	0.0407	12.50	18.2	5.250	0.218
C	1.07	87.2	64.4	412	120	0.0533	10.10	13.7	4.700	0.233

From the viewpoint of the influence on the ferrite, we divide the R ions studied into two categories:

(1) the R ions with a radius very close to those of the Ni and Fe ions, which can enter into the spinel lattice;

(2) the R ions which have an ionic radius larger than those of the metallic ions of the spinel lattice; during the sintering process some of these ions will diffuse to the grain boundaries and form an isolating ultra-thin layer around grains.

Figure 1 shows the Curie temperatures T_C and the specific saturation magnetizations σ_s measured at 77 and 293 K for the $Ni_{0.7}Zn_{0.3}Fe_{1.98}R_{0.02}O_4$ samples in order of increasing R ion radius.

All compositions, irrespective of R ion type, have nearly the same Curie point, which confirms that in these compounds the Fe–Fe interactions dominate. The small quantity of R_2O_3 in these compounds only slightly influences T_C. However, the Curie temperatures are a little lower than that of Ni–Zn ferrite without R owing to a decrease in the Fe–Fe interaction number. A larger decrease in T_C was obtained for the samples with Er and Dy which have a small ionic radius, because the R–Fe interaction decreases with increasing ionic radius, when R ions enter into the spinel lattice. The Curie temperature for the ferrite without R is 415 °C and for that containing Er is 405 °C; the slight difference explains the minor influence of R–Fe interactions at high temperatures.

The specific magnetization measured at 77 K is to some extent variable. It is about 92 emu g^{-1} for R ≡ Yb, Dy and Tb, rising to about 100–103 emu g^{-1} for Er and

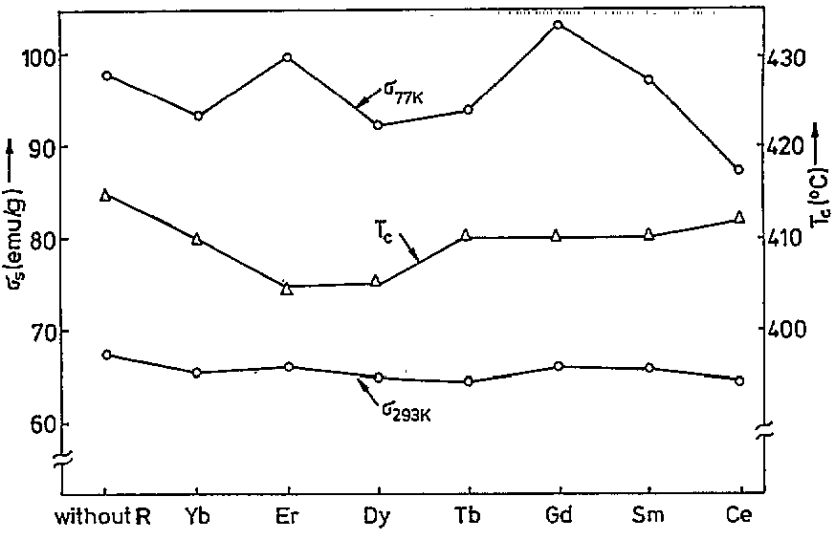

Figure 1. Curie temperature and specific saturation magnetization at liquid-nitrogen temperature and room temperature for $Ni_{0.7}Zn_{0.3}Fe_{1.98}R_{0.02}O_4$ samples, with R ≡ Yb, Er, Dy, Tb, Gd, Sm, or Ce.

Gd. We think that the Er and Gd ions become ferromagnetically ordered, and the others antiferromagnetically ordered. In this case we suppose that a small component of the magnetic moment is induced by the R–Fe interaction, owing to the ferromagnetic ordering of the rare-earth ion moments at low temperatures, when these ions enter in the spinel lattice (this is the case for Er ions) [10]. This interaction causes the rare-earth magnetism at room temperature and above [11]. The Gd ions, because of their large ionic radius, enter only partially into the lattice; the rest form the orthoferrite $GdFeO_3$ with Fe^{3+} ions. The higher value of σ_s for Gd substitution may be explained by a modified distribution of the rest of the Fe^{3+} ions on the two sublattices compared with their distribution in the ferrite without substitutions. For $Ni_{0.7}Zn_{0.3}Fe_{1.98}Ce_{0.02}O_4$, σ_s (77 K) has the lowest value, about 87 emu g^{-1}, and T_C is the highest. This peculiarity could be associated with the fact that Ce is a non-typical R element having a broader width of the 4f band and, consequently, gives rise to a strong hybridization of the 4f states with the 3d band [12]. At 290 K, σ_s has nearly the same value for all samples with R ions; it is slightly smaller than that for pure ferrite.

An interesting result was obtained concerning the temperature dependence of the initial permeability. Figure 2 shows the curves of permeability μ_i versus temperature T.

One should note the following.

(a) The R ion influences the shape of the $\mu_i(T)$ curves. For all samples containing rare-earth ions, except Ce, the curves show a plateau, which extends over a temperature range whose width depends on the R ion type. In this region, μ_i is almost independent of temperature, the relative variation of permeability $\Delta\mu_i/\mu_i$ being about 1–2%.

(b) The magnitude of the permeability increases with increasing R ionic radius.

(c) For Ce substitution, the initial permeability increases continuously with increasing temperature up to the Curie point.

To explain the shape of the $\mu_i(T)$ curves we can recollect here that, for a ferrite with a given chemical composition, the value of the crystal anisotropy constant K_1 is composed

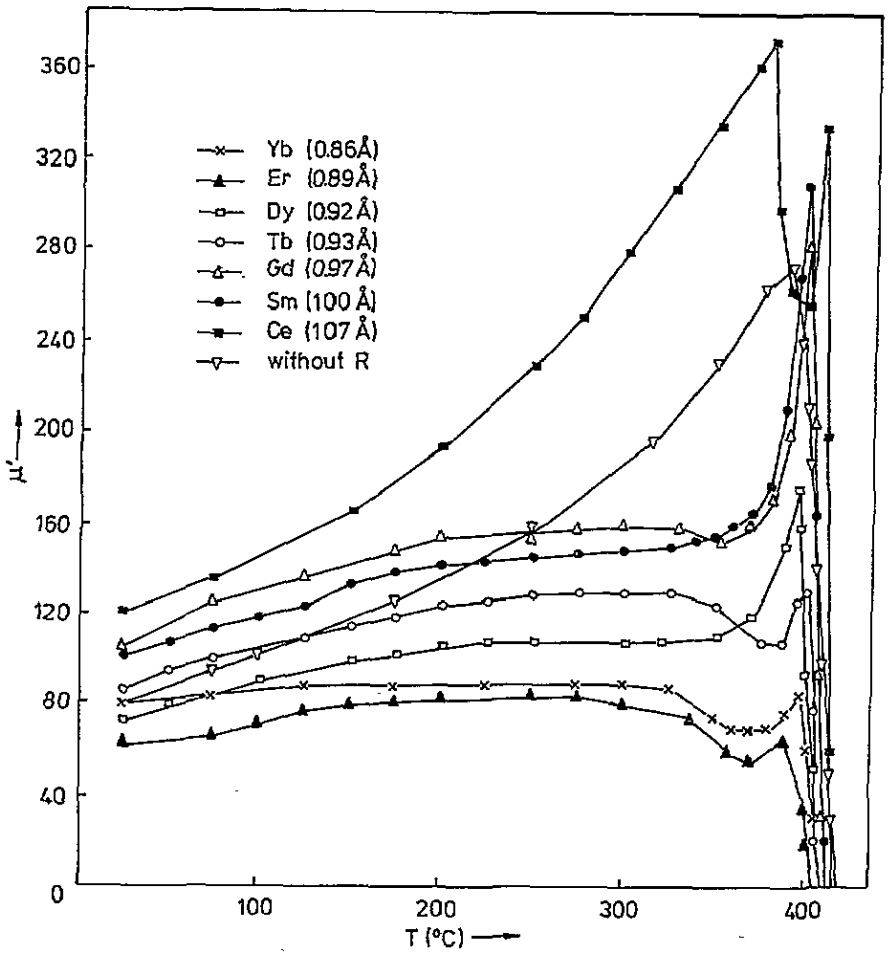

Figure 2. Initial magnetic permeability as a function of temperature for $Ni_{0.7}Zn_{0.3}Fe_{1.98}R_{0.02}O_4$ samples. The rare-earth ionic radii are shown in parentheses.

of the contributions of the individual magnetic ions [13]. In our ferrites, the contribution of Fe^{3+} ions to K_1 is negative, while that of the Ni^{2+} ions on octahedral sites can be neglected [14] and K_{1R} is positive [15, 16]. Furthermore, we suppose that the Fe^{2+} ions which appear during the sintering process can occupy both the octahedral (B) and the tetrahedral sites (A) in ferrites [1] and, as shown previously [17], their contributions to the anisotropy constant K_1 have opposite signs: $K_1(Fe^{2+}(B)) < 0$ and $K_1(Fe^{2+}(A)) > 0$. The temperature dependence of all these contributions to K_1 can explain the appearance of the plateaux in the $\mu_i(T)$ curves, which is of a great technical importance. On the other hand, the shape of the $\mu_i(T)$ curves can be correlated with the microstructure of the material. All microstructural factors such as the size and form of the crystallites, the structure of the grain interfaces, the precipitates, the inhomogeneities, the cationic and anionic vacancies and the dislocations, can finally lead to the statistical composition differences determining a dispersion of the K_1 compensation temperature and, therefore, a flattening of the $\mu_i(T)$ curves.

In figure 3 the initial magnetic permeability and the average grain size D_m are given for all samples. We explain the observed influence of the R ion type on the value of μ_i as

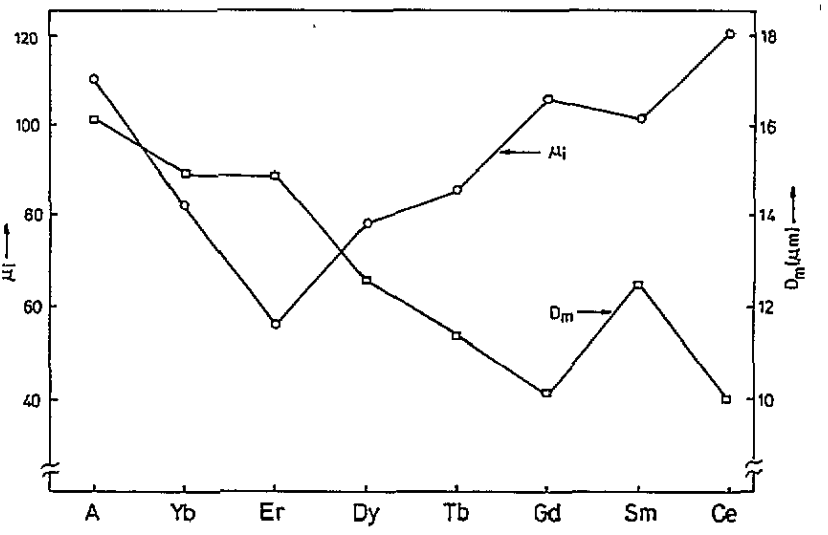

Figure 3. Initial magnetic permeability and average grain size as functions of the species of rare-earth ions.

an effect of the ionic radius size.

From figure 3, one can see that the value of μ_i decreases for R ions with small radius but increases with increasing radius of the R ions.

The R ions which enter into the spinel lattice, owing to their electronic configuration, will distort the lattice or crystalline field, generating an internal stress that will hinder the domain wall displacement and, as a consequence, the permeability will decrease.

The R ions which enter into the lattice only partially, during the sintering process, will diffuse to the grain boundaries and form an isolating ultra-thin layer around the grains. This segregation process impedes the displacement of grain boundaries and further crystal growth is stemmed [18]. This results in quite small grains, with a reduced number of inner pores. In this case the displacement of the magnetic domain walls becomes easier and a larger μ_i will be obtained.

From figure 3, one can observe the decrease in the average grain size D_m with increasing ionic radius. However, for the Sm_2O_3 substituent, the value of D_m is a little larger than those of neighbouring R substituents. Probably, during the sintering process, SmO_2 could also appear, which acts as a flux owing to its low melting point (642 °C) and which can favour the growth of lower grains with inner pores. Other crystallites in these samples will grow freely or will be stopped by the segregated layer. In consequence, the structure of the resulting ferrite presents very heterogeneous grains and a significant porosity, especially intergranular, that will therefore lead to a slight decrease in permeability [19].

Unfortunately, the permeabilities for samples with R_2O_3 are not large compared with those of the sample without R_2O_3, since part of the initial iron oxide was substituted by R_2O_3 and another part formed a weak magnetic compound $RFeO_3$ with R_2O_3.

Our assumption concerning the role of the R ion radius is confirmed by the lattice constant measurements given in table 1. We observe that the lattice parameters are not constant but increase when the R ions enter into the spinel lattice and begin to decrease for a large difference between the cation radii of R^{3+} and Fe^{3+} owing to the removal of the rare-earth ions from the spinel lattice. One can see that for Ce and Gd substitutions

the lattice constants are a little smaller than that of unsubstituted Ni–Zn ferrite. For these substitutions it is possible that the spinel lattice is slightly compressed by the resulting precipitate.

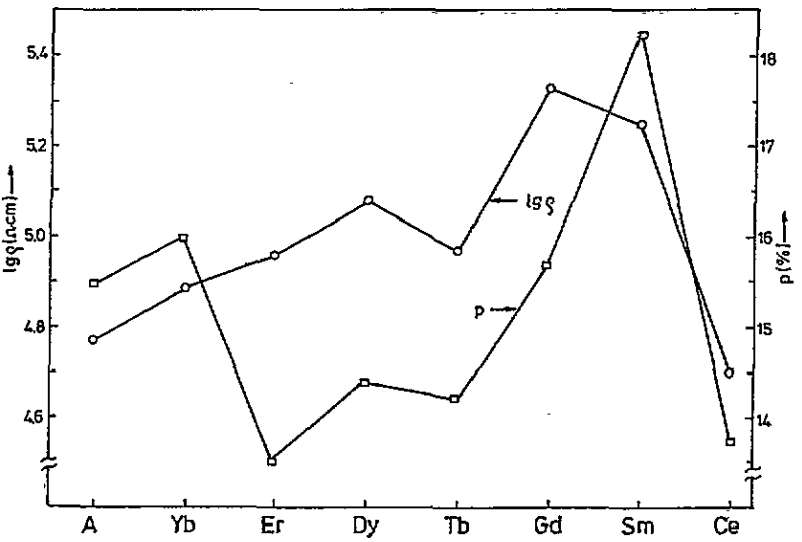

Figure 4. Porosity and electrical resistivity at room temperature as functions of the species of rare-earth ions.

Figure 4 shows the influence of the R ion on the electrical resistivity and the porosity. The samples are generally porous; the highest porosity was obtained for the substituted Sm sample for the reason given above. Also, one can see that all rare-earth oxides, except for Ce_2O_3, increase the electrical resistivities as the result of the formation of insulating intergranular layers ($RFeO_3$ contains Fe^{3+} ions only).

However, it has been noted that one cannot establish a correlation between the resistivity of the specimens and their Fe^{2+} ion concentration because, in the conduction process, Fe^{2+} ions on only the octahedral sites participate [20] or it is assumed [1] that the Fe^{2+} ions can occupy both the octahedral and the tetrahedral sites. For instance, from table 2, one can see that the ferrites which contain R ions with a large radius (Gd, Sm or Dy), even if they contain a large quantity of Fe^{2+}, have a high resistivity. On the one hand, the formation of insulating intergranular layers impedes the oxidation of Fe^{2+} ions inside the grains during slow cooling of the samples and, on the other hand, it increases the resistivity of the material.

From table 2 it can be observed that the Tb-substituted ferrite contains the highest Fe^{2+} amount and it has a small resistivity. A possible cause of this result could be the generation at a high temperature (1300 °C) of Tb^{4+} ions from Tb^{3+} ions which having a smaller radius (0.76 Å) can substitute for Fe^{3+} ions on octahedral sites. Also, Satbir *et al* [21] have supposed that the introduction of a high-valence cation, such as Me^{4+}, in the lattice of a Ni–Zn ferrite generates Fe^{2+} ions. In the present case, the Tb^{4+} ions will generate Fe^{2+} on octahedral sites that will participate in the conduction process; at the same time, a marked increase in the Fe^{2+} content is noted. The small value of ρ for Ce may be attributed to Ce valence fluctuation between the Ce^{3+} and Ce^{4+} ions.

To obtain complete information on the effect of the R ion on the conduction process the temperature dependence of ρ was measured between room temperature and the Curie point.

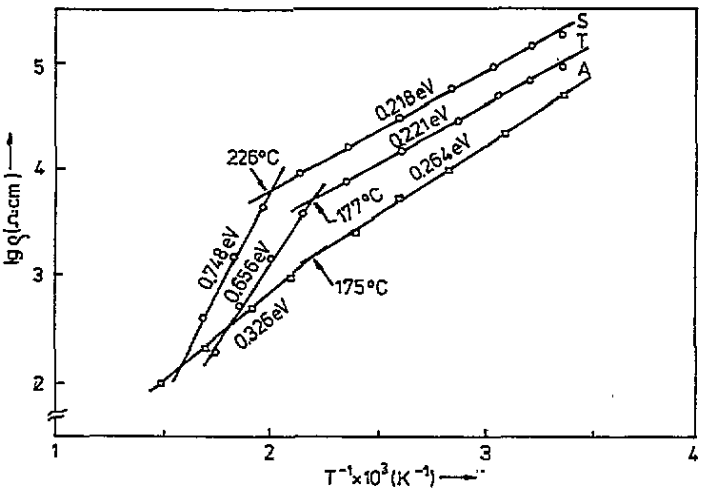

Figure 5. Logarithm of the electrical resistivity versus reciprocal temperature for the three samples studied.

The variation in the logarithm of electrical resistivity as a function of reciprocal temperature for three samples is plotted in figure 5. One can note the following.

(a) For all samples, irrespective of whether they contain an R ion or not there are, in the temperature interval investigated, two regions with completely different activation energies.

(b) The change in the slope of the $\log[\rho(1/T)]$ curve takes place at around the temperature of 200 °C. The steeper slopes of the straight lines for higher temperatures can be regarded as due to thermally activated mobility of the charge carriers, but not to a thermally activated creation of these carriers. Conceptually, this would provide a simple explanation for the strong increase in conductivity at a higher temperature.

(c) In the temperature interval investigated, ρ decreases by about two orders of magnitude.

(d) All curves can be described by the following equation:

$$\rho = A_1 \exp(E_1/kT) + A_2 \exp(E_2/kT). \tag{1}$$

The constants A_1 and A_2 can be computed by extrapolating to infinite temperature; E_1 and E_2 are the activation energies for the two temperature intervals; k is the Boltzmann constant.

(e) The difference between the R substituents is in the value of ρ only, while the activation energies evaluated for each interval do not differ so much. In table 2 are given the activation energies calculated for the first temperature interval, from the formula

$$E_1 = 0.198 \times 10^{-3} \frac{\delta(\log \rho)}{\delta(1/T)} \qquad \text{(eV)}. \tag{2}$$

The small values for the activation energies confirm the electronic character of the conduction process that consists in the hopping of electrons between Fe^{2+} and Fe^{3+} ions,

statistically situated on octahedral spinel sites ('hopping process') [20]. The values of the activation energies are independent of the R ion type and the Fe^{2+} concentration clearly shows that the activation energy is determined by the mobility of the carriers and not their concentration.

(f) Also, from figure 5, one can observe that the jump in the activation energy given by $\Delta E = E_2 - E_1$ is larger for R-contaminated samples than for the sample without R. This result suggests the existence of a conduction sensitive to structure. In other words, the presence of the crystallites with a spinel structure with an insulating shell can affect the electrical properties of the material.

(g) On the other hand, it should be noted that the temperature of the discontinuity in the $\log[\rho(1/T)]$ curve approximately coincides with the temperature at which the plateau in the $\mu_i(T)$ curve starts. This result allows us to conclude that both the electrical and the magnetic properties are largely determined by the same 3d electrons of the iron ions, which are carriers of both the electrical charge and the spin magnetic moment.

4. Conclusions

The above results reveal several facts which are noteworthy.

(1) The influence of the R ions on the properties of an Ni–Zn ferrite can be explained as the effect of their ionic radius.

(2) The substitutions of iron ions by rare-earth ions provide clearly improved temperature characteristics of the initial permeability.

(3) Also, there was evidence that the permeability is not dependent on porosity; the different values of the μ_i can be explained by the difference between the average sizes of the grains. To obtain a higher permeability in our case, the ferrites must be produced such that grains with a narrower range of diameters (about 10 μm) are obtained.

(4) It is possible to increase the electrical resistivity by using a small quantity of R_2O_{03} substituent owing to the structural heterogeneity generated by the insulating intergranular layers. The isolation of a grain by high-resistance ultra-thin layers of $RFeO_3$ orthoferrite is seen as one of the most promising approaches for further reduction in the eddy current losses at the higher operating frequencies.

(5) From the viewpoint of effectiveness, the R ions with a large radius and with a stable valence of 3+ are found to be the best substituents for improvements in the magnetic and electrical properties of the soft magnetic Ni–Zn ferrite. In our work, Gd_2O_3 is preferred of the seven rare-earth oxides investigated.

References

[1] Rezlescu E, Rezlescu N, Pasnicu C and Craus M L 1993 *Ceram. Int.* **19** 71
[2] Rezlescu E, Rezlescu N, Pasnicu C, Craus M L and Popa D P 1992 *J. Magn. Magn. Mater.* **117** 448
[3] Yang Ying-chang, Kong Lin-shu, Zha Yuan-bo, Sun Hong and Pei Xie-di 1988 *J. Physique Coll.* **49** C8 543
[4] Li Hong-shuo, Hu Bo-ping and Coey J M D 1988 *Solid State Commun.* **66** 133
[5] Yang Ying-chang, Kong Lin-shu, Sun Shu-he and Gu Dong-mei 1988 *J. Appl. Phys.* **63** 3702
[6] Rezlescu N and Rezlescu E 1993 *Solid State Commun.* **88** 139
[7] Merceron T 1965 *Ann. Phys.* **10** 121
[8] Inui T and Ogasawara N 1977 *IEEE Trans. Magn.* **MAG-13** 1729
[9] Craus M L, Rezlescu E and Rezlescu N 1992 *Phys. Status Solidi* a **133** 439
[10] Bozorth R M 1958 *Phys. Rev. Lett.* **1** 362

[11] Gavigan J P and Givord D 1990 *J. Magn. Magn. Mater.* **84** 288
[12] Rastogi A K, Hilscher G, Gratz E and Pillmayr N 1988 *J. Physique Coll.* **49** C8 277
[13] Broese van Groenou A and Schulkes I 1967 *J. Appl. Phys.* **38** 1133
[14] Miyata N 1961 *J. Phys. Soc. Japan* **16** 1291
[15] Maruyama H, Yamazaki H, Givord D, Gavigan J, Li H-S, Sagawa M and Hirosawa S 1988 *J. Physique Coll.* **49** C8 563
[16] Li Hong-shuo, Hu Bo-ping, Gavigan J P, Coey J M D, Pareti L and Moze O 1988 *J. Physique Coll.* **49** C8 541
[17] Potakova V A, Romanov V P, Zverev N D, Gromovenco O I and Rubalskaya E V 1971 *Phys. Status Solidi* a **4** 327
[18] Paulus M 1962 *Phys. Status Solidi* **2** 1325
[19] Globus A 1963 *Thesis* Université de Paris
[20] Smit J and Wijn H P J 1961 *Les Ferrites* (Paris: Dunod)
[21] Satbir S, Tripathi R B and Das B K 1987 *Phys. Status Solidi* a **100** k185